Electronic Supplementary Material (ESI) for Sustainable Energy & Fuels.

Supplementary Information

Phosphorization of Prussian Blue Analogue-derived Co-N-C Catalyst for Synchronously Boosting the Oxygen Reduction And Evolution Reactions

Xiangyang Zhou, Lei Xu, Yuning Gao, Liang Li, Jingjing Tang*, Juan Yang*

School of Metallurgy and Environment, Central South University, Changsha 410083, China

*Corresponding author: Jingjing Tang, Juan Yang

E-mail: tangjj@csu.edu.cn; j-yang@csu.edu.cn

Phone: +86-731-88836329; Fax: +86-731-88871017

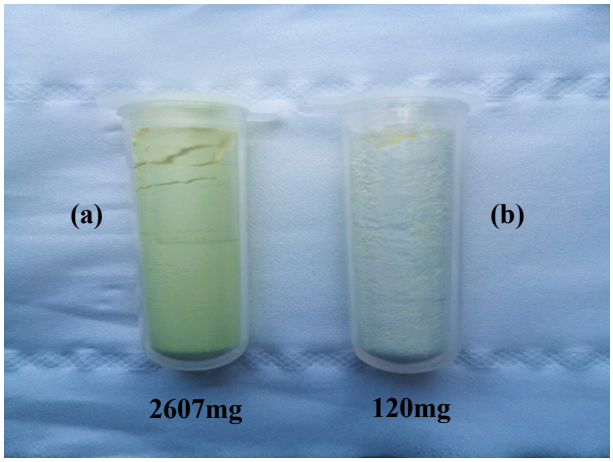

Figure S1. Photographs of (a) Bulk g-C_3N_4 and (b) GCNS

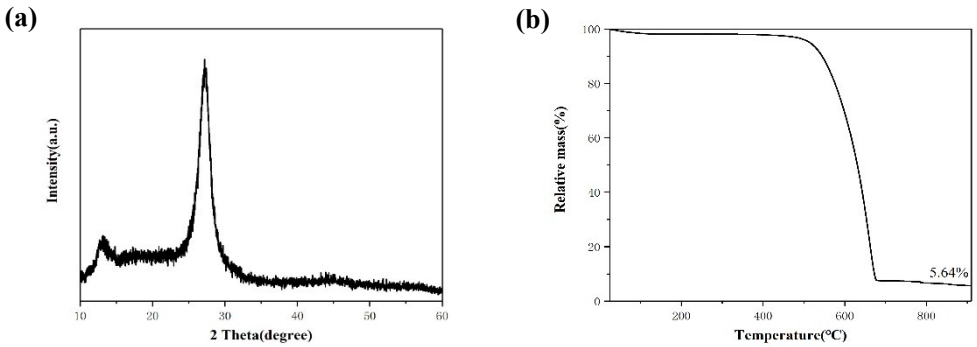

Figure S2. (a) XRD pattern of GCNS and (b) TGA curve of GCNS under Ar.

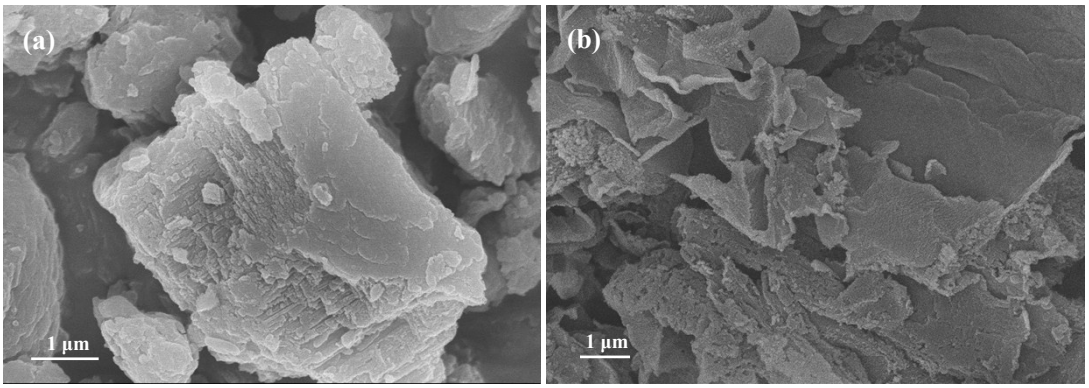

Figure S3. SEM images of (a) Bulk g-C_3N_4 and (b) GCNS.

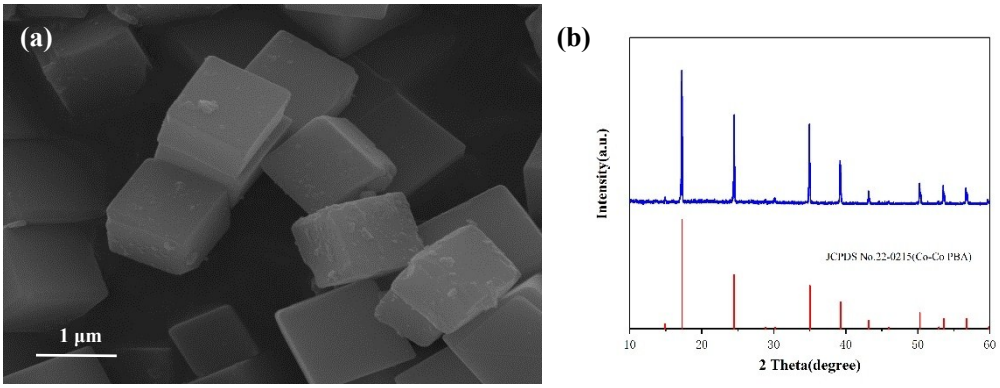

Figure S4. (a) SEM image of CoCo-PBA and (b) XRD pattern of CoCo-PBA.

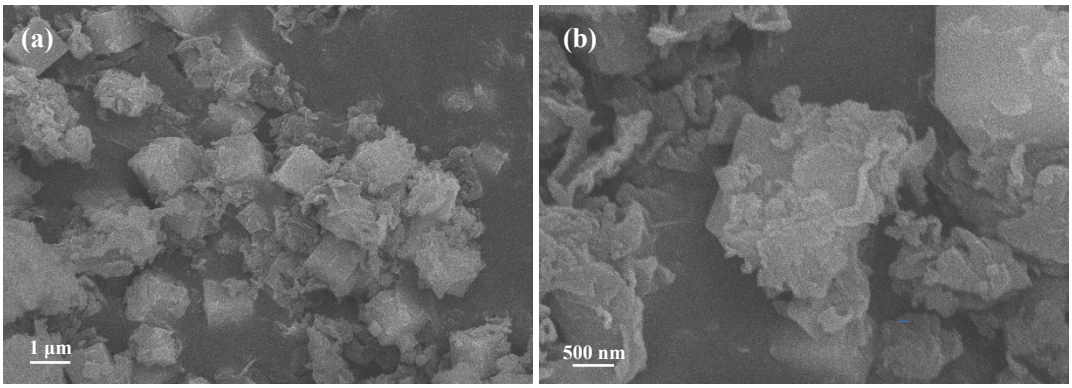

Figure S5. SEM images of CoCo-PBA@GCNS.

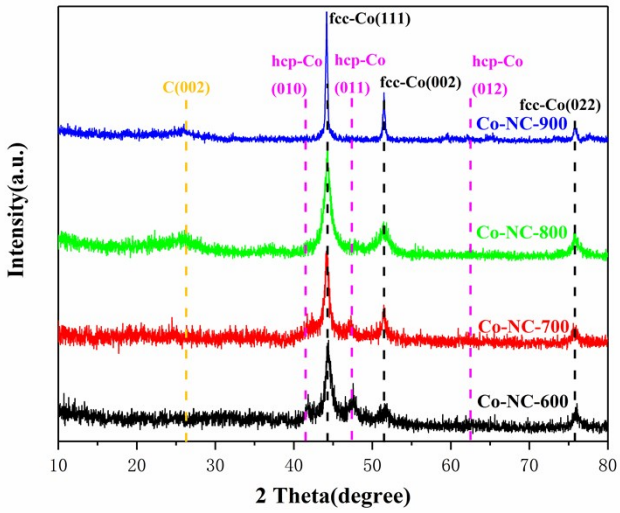

Figure S6. XRD patterns of the Co-NC-T catalysts obtained at different temperatures from 600 to 900℃.

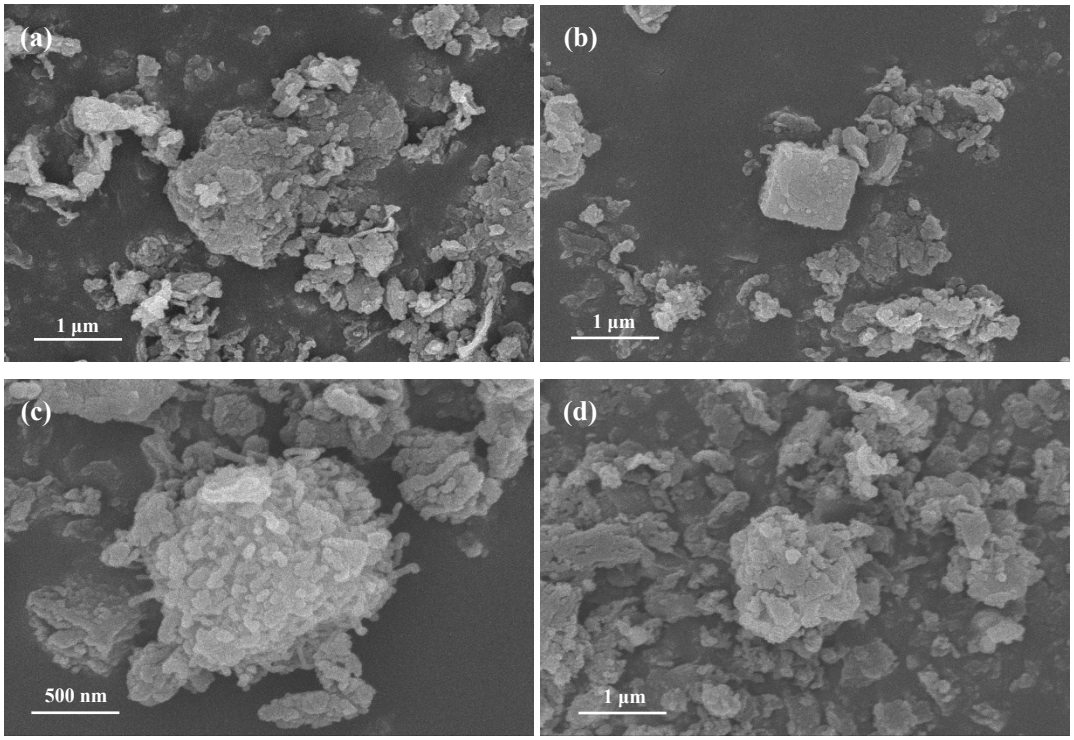

Figure S7. SEM images of the (a) Co-NC-600, (b) Co-NC-700, (c) Co-NC-800 and (d) Co-NC-900.

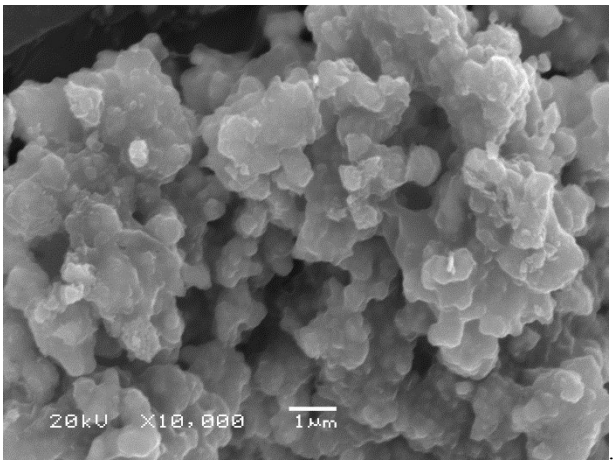

Figure S8. SEM image of the PBA-800.

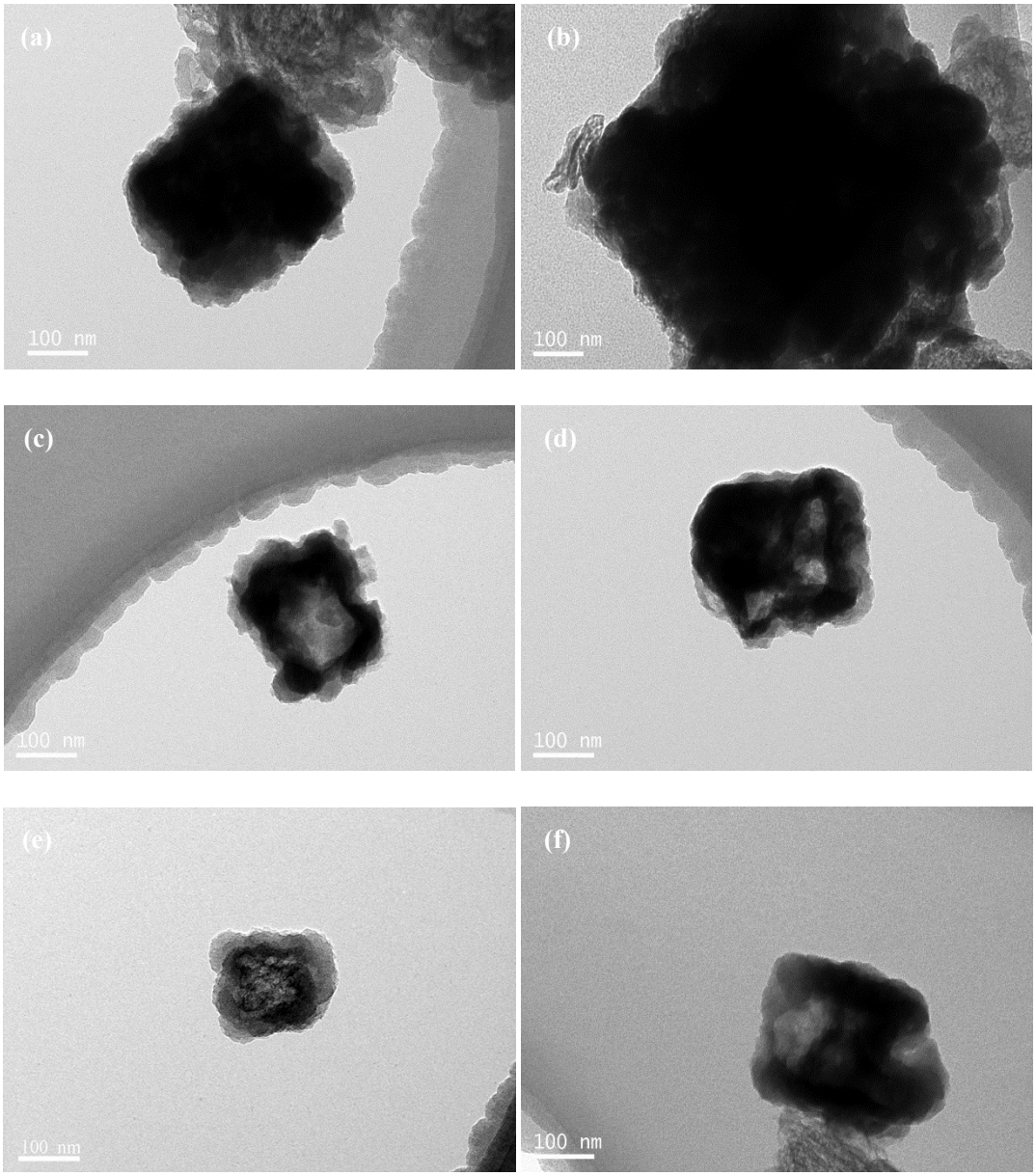

Figure S9. TEM images of CoP-NPC (a-b) defects; (c-d) cavities; (e-f) broken.

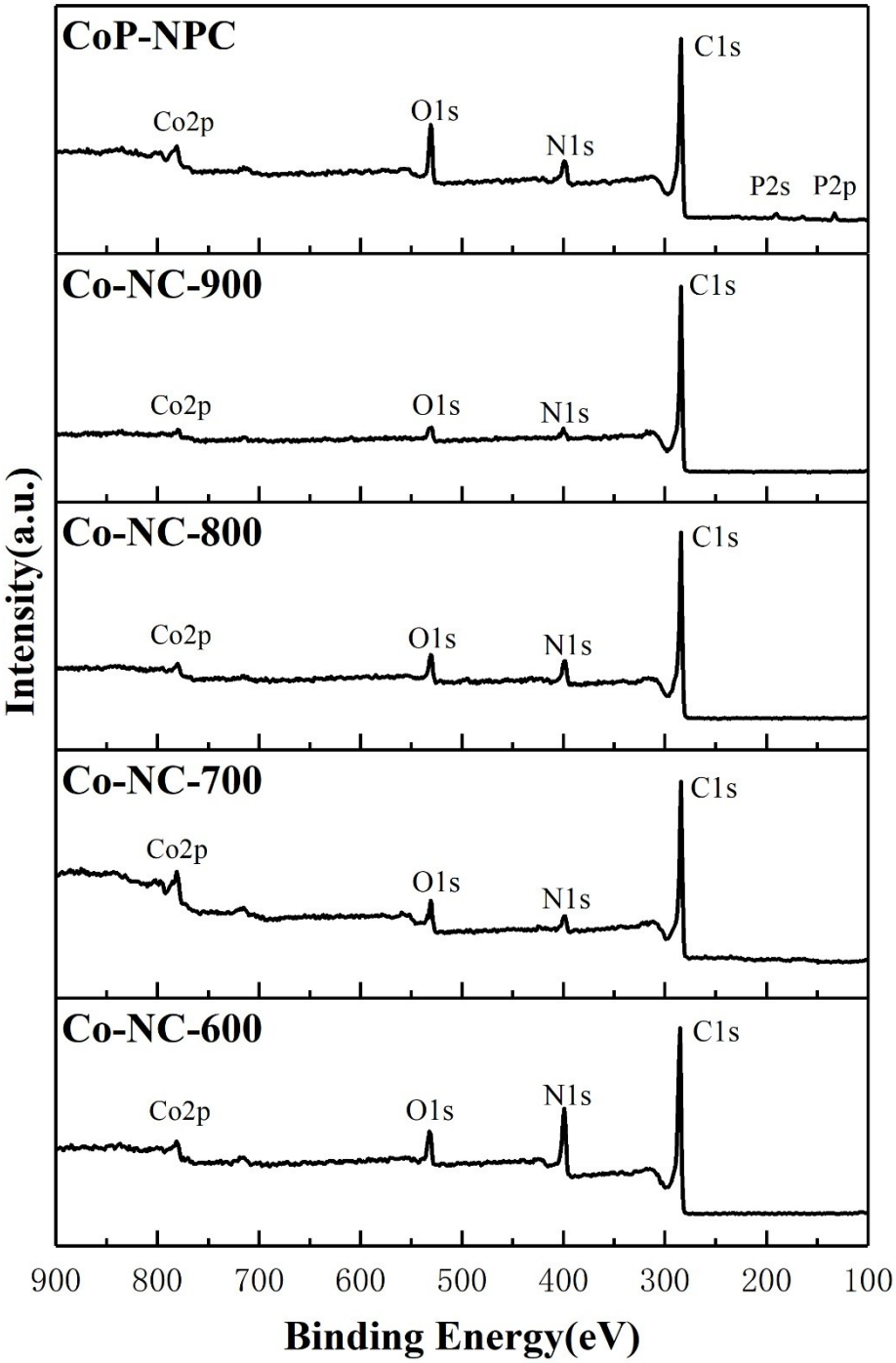

Figure S10. XPS survey spectra of the CoP-NPC and Co-NC-T catalysts obtained at (A) 600℃, (B) 700℃, (C) 800℃, (D) 900℃

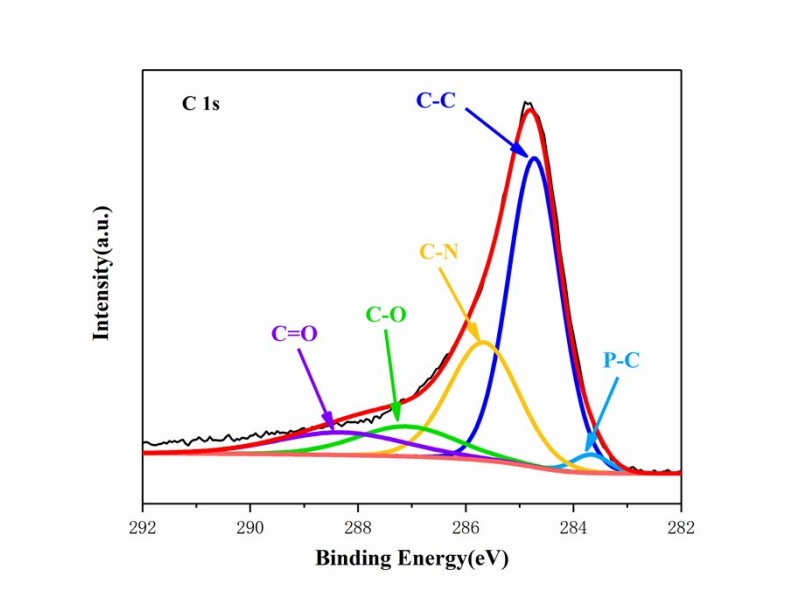

Figure S11. High-resolution C 1s XPS spectra of the CoP-NPC**.**

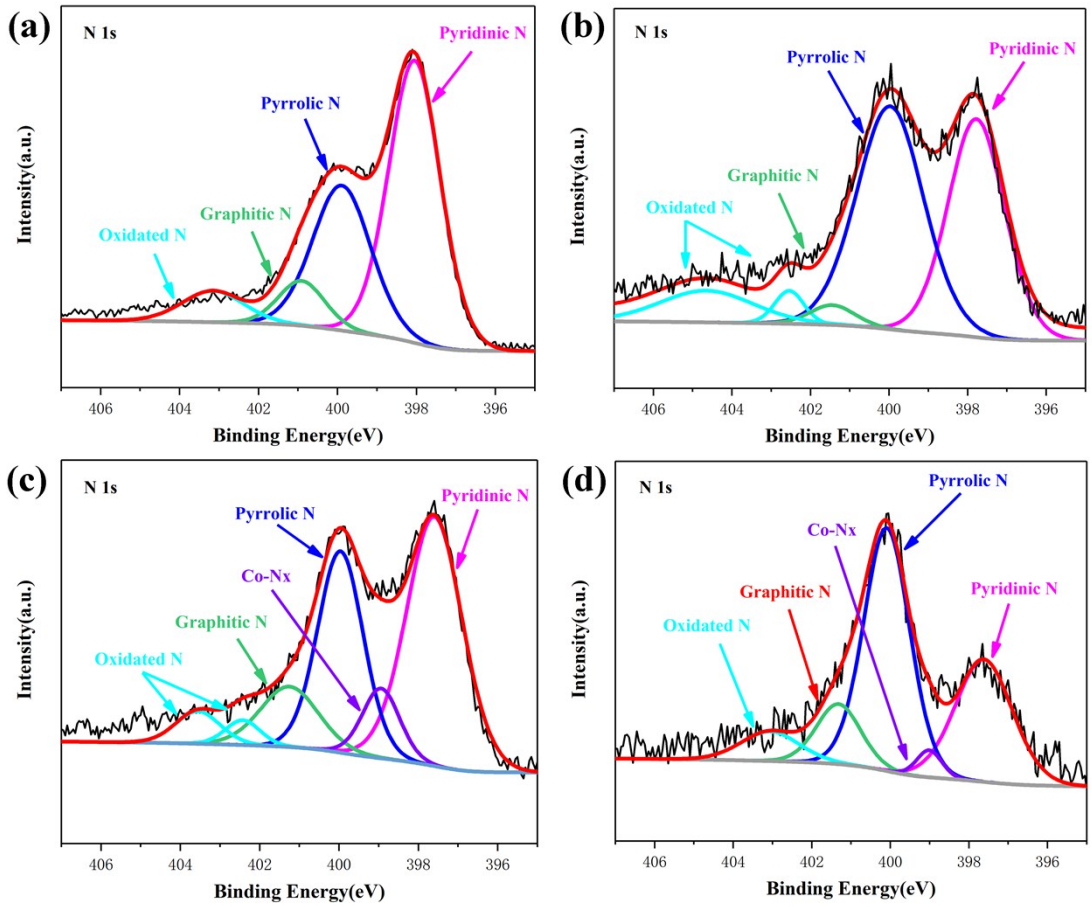

Figure S12. High-resolution N 1s XPS spectra of Co-NC-T obtained at (a) 600℃, (b) 700℃, (c) 800℃, (d) 900℃.

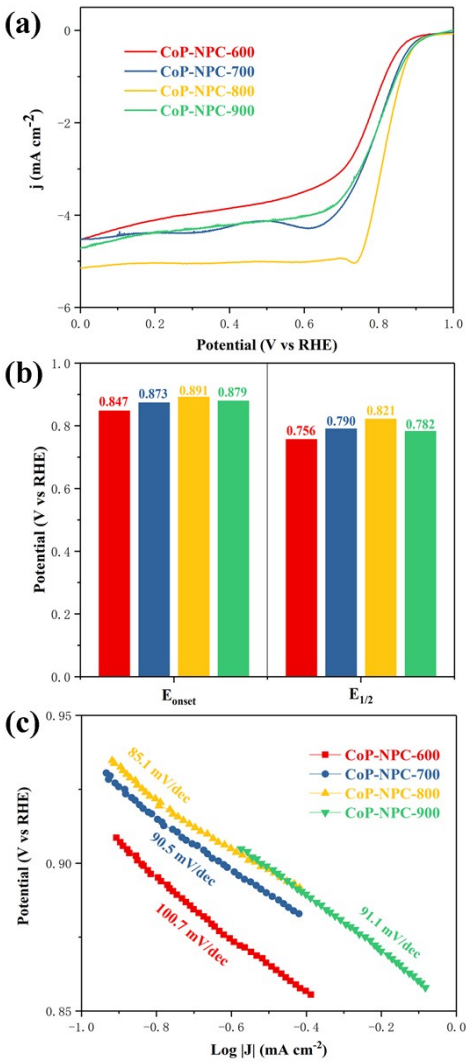

Figure S13. (a) LSV curves of CoP-NPC-T (T=600℃, 700℃, 800℃, 900℃); (b) Bar plots of E_{onset} and $E_{1/2}$; (c) Tafel plots of different samples.

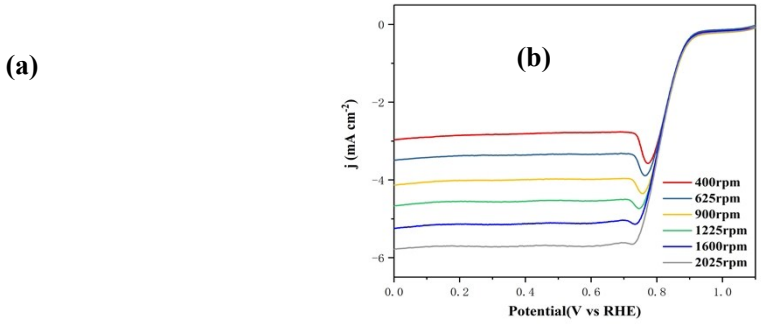

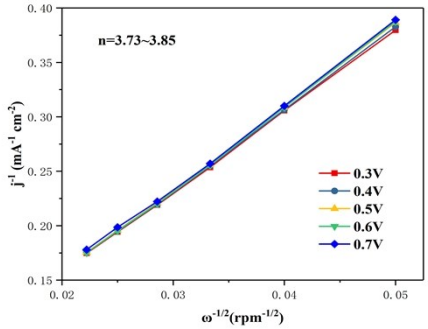
n=3.73~3.85
0.3V
0.4V
0.5V
0.6V
0.7V
j⁻¹ (mA⁻¹ cm⁻²)
ω⁻¹/²(rpm⁻¹/²)

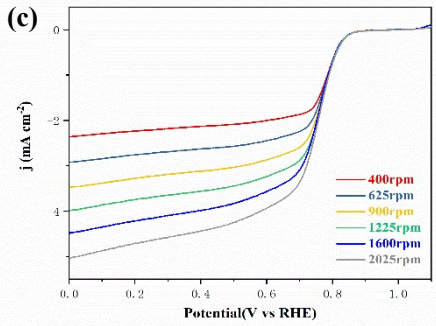
(c)
400rpm
625rpm
900rpm
1225rpm
1600rpm
2025rpm
j (mA cm⁻²)
Potential(V vs RHE)

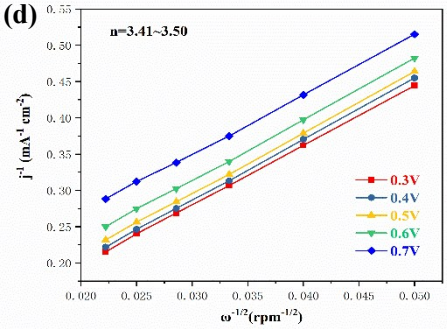
(d)
n=3.41~3.50
0.3V
0.4V
0.5V
0.6V
0.7V
j⁻¹ (mA⁻¹ cm⁻²)
ω⁻¹/²(rpm⁻¹/²)

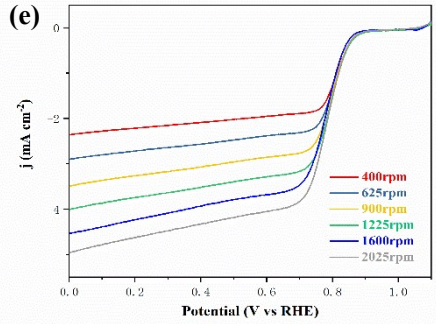
(e)
400rpm
625rpm
900rpm
1225rpm
1600rpm
2025rpm
j (mA cm⁻²)
Potential (V vs RHE)

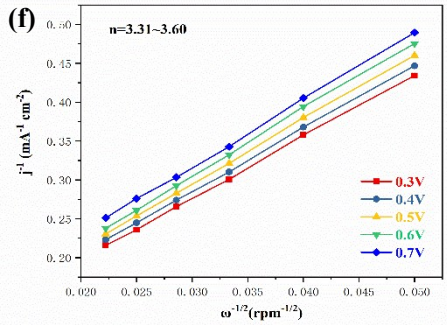
(f)
n=3.31~3.60
0.3V
0.4V
0.5V
0.6V
0.7V
j⁻¹ (mA⁻¹ cm⁻²)
ω⁻¹/²(rpm⁻¹/²)

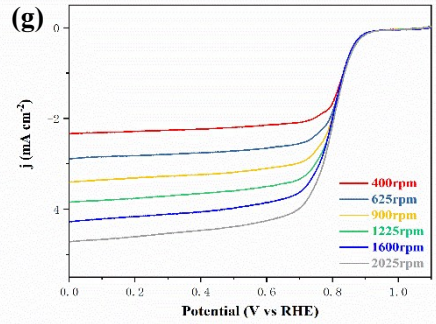
(g)
400rpm
625rpm
900rpm
1225rpm
1600rpm
2025rpm
j (mA cm⁻²)
Potential (V vs RHE)

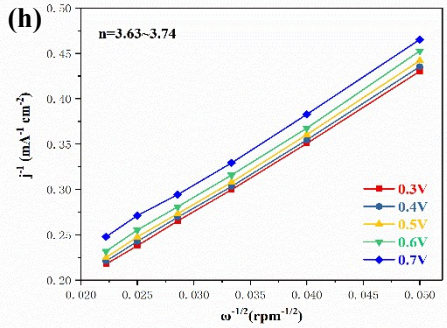
(h)
n=3.63~3.74
0.3V
0.4V
0.5V
0.6V
0.7V
j⁻¹ (mA⁻¹ cm⁻²)
ω⁻¹/²(rpm⁻¹/²)

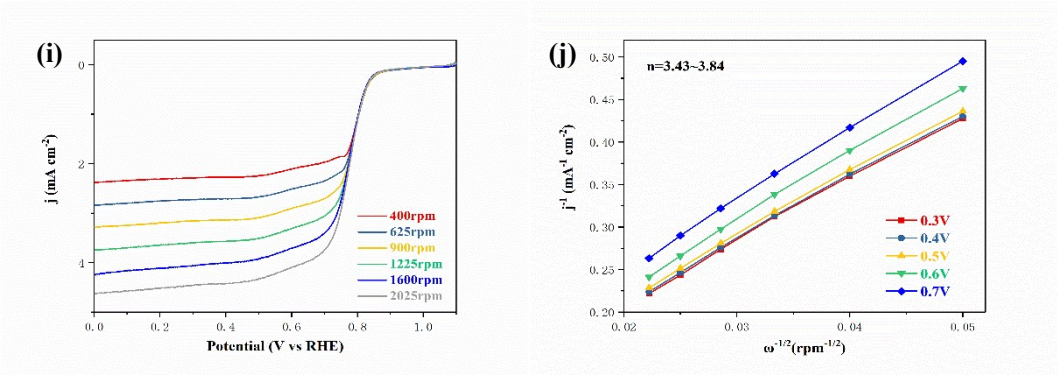

Figure S14. LSV curves of (a) CoP-NPC and the Co-NC-T obtained at (c) 600℃, (e) 700℃, (g) 800℃, (i) 900℃ at different rotating speeds; K-L plots for (b) CoP-NPC and the Co-NC-T obtained at (d) 600℃, (f) 700℃, (h) 800℃, (j) 900℃.

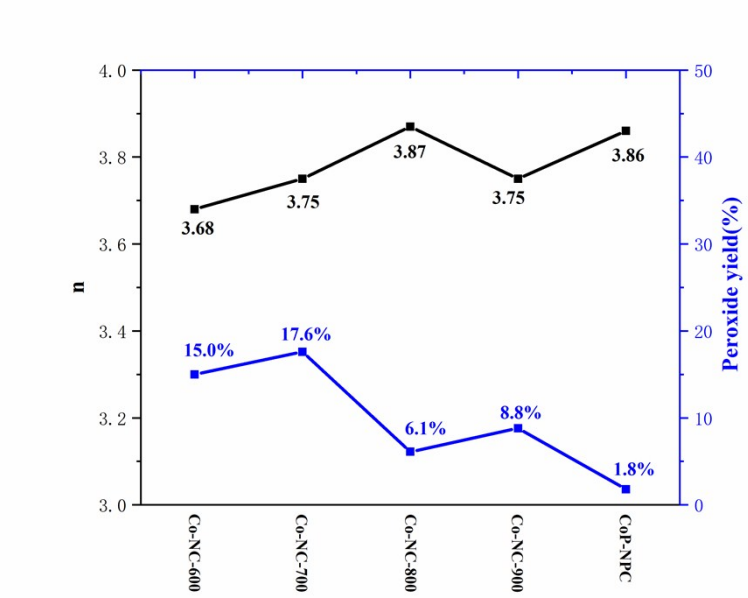

Figure S15. Peroxide yield (blue) with regard to the total oxygen reduction products and the electron-transfer number (n) (black) of samples in O_2-saturated 0.1M KOH at 1600rpm.

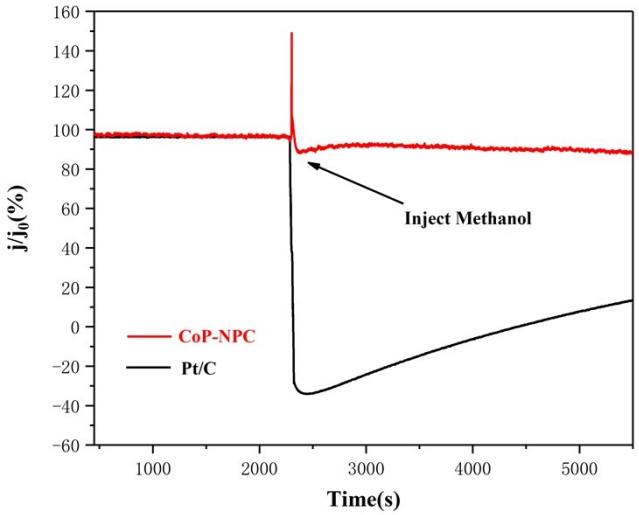

Figure S16. Methanol crossover tolerance test of CoP-NPC and Pt/C conducted by chronoamperometry measurement;

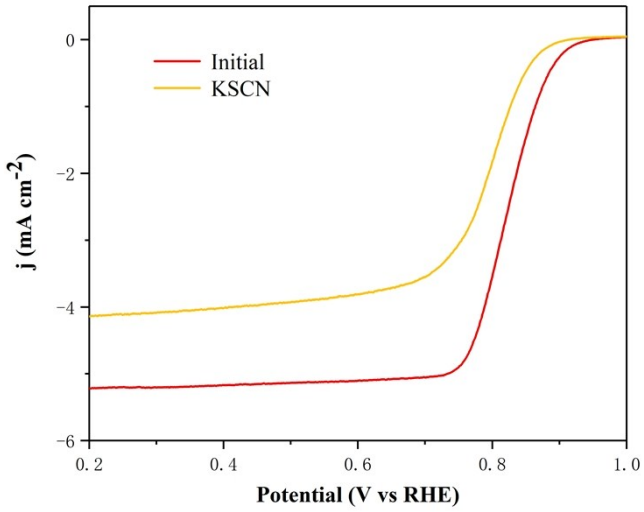

Figure S17. Effect of KSCN addition on the electrocatalytic activity of CoP-NPC.

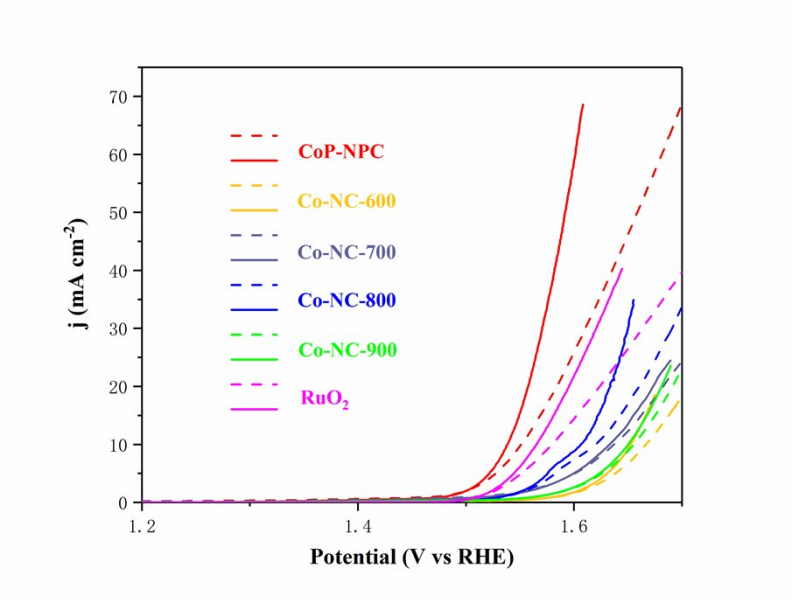

Figure S18. The LSV curves of Co-NC-T (600℃, 700℃, 800℃, 900℃), RuO_2 and CoP-NPC with IR-correction (solid line) and without IR-correction (dashed line).

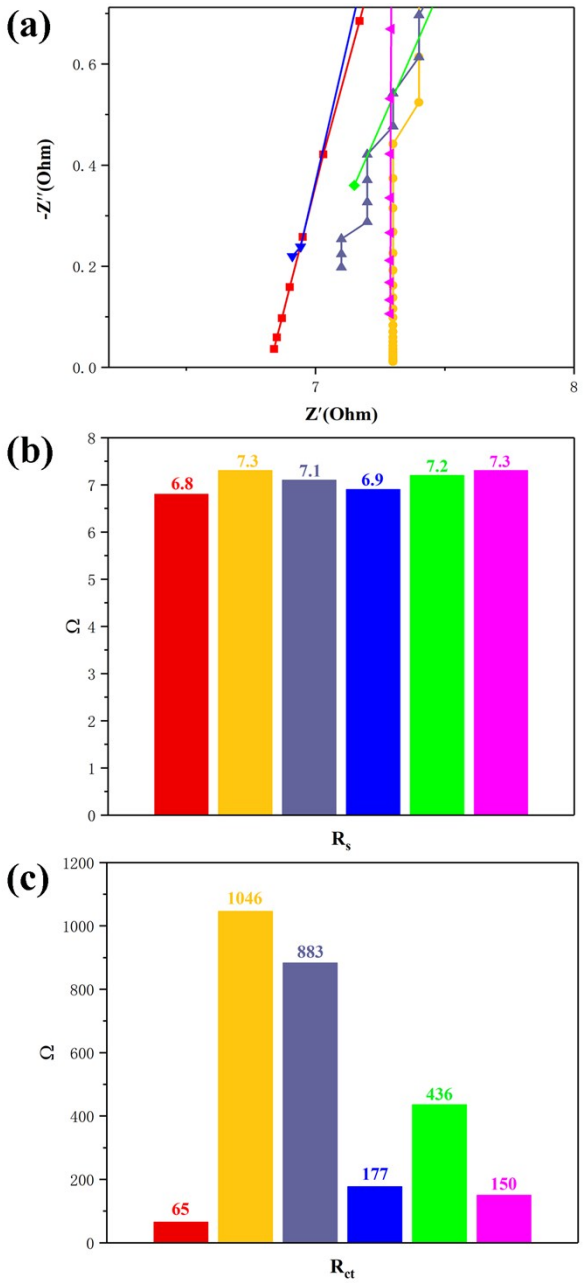

Figure S19. (a) The zoomed view of the plots in the high frequency regions; (b) The R_s and (c) R_{ct} values of CoP-NPC, Co-NC-T (600℃, 700℃, 800℃, 900℃) and RuO_2.

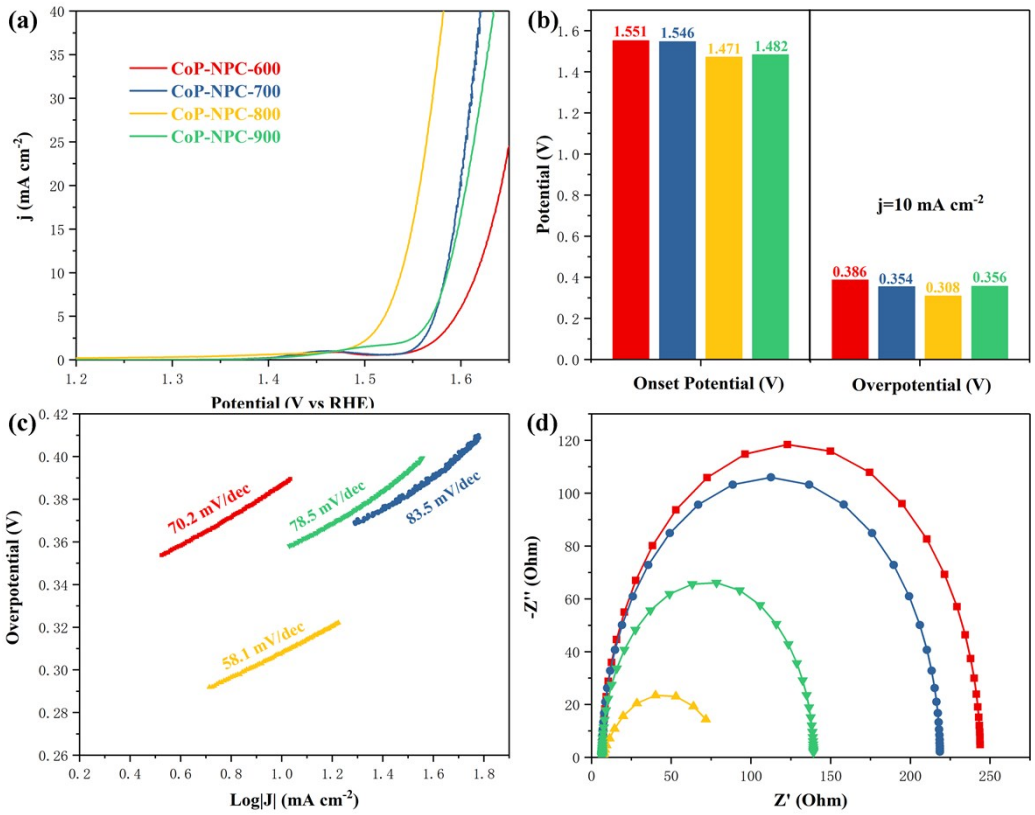

Figure S20. (a) OER LSV curves with IR_s-correction; (b) Overpotentials and the onset potentials of different samples; (c) Tafel plots of different samples; (d) Nyquist plots of different samples.

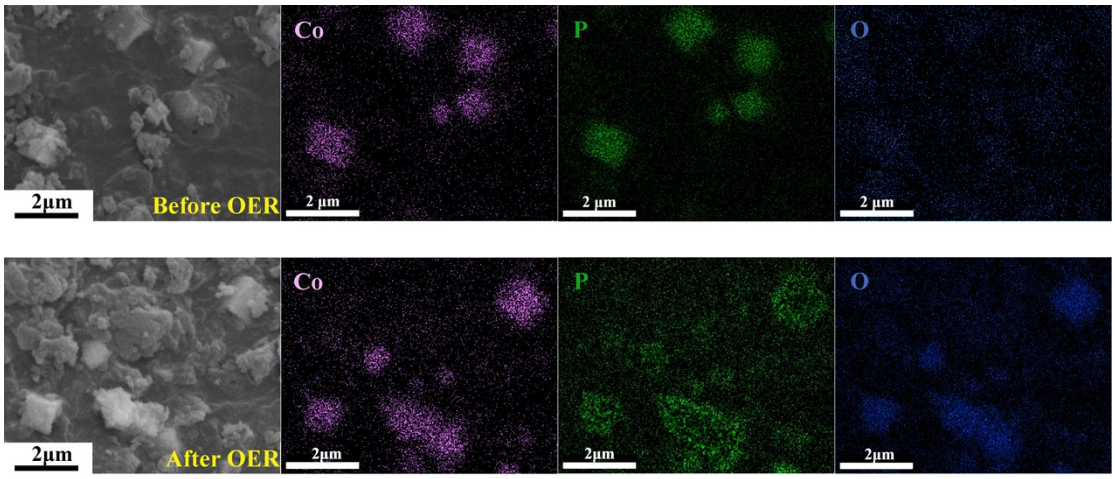

Figure S21. SEM images and corresponding elemental mapping before and after OER stability test in 1M KOH.

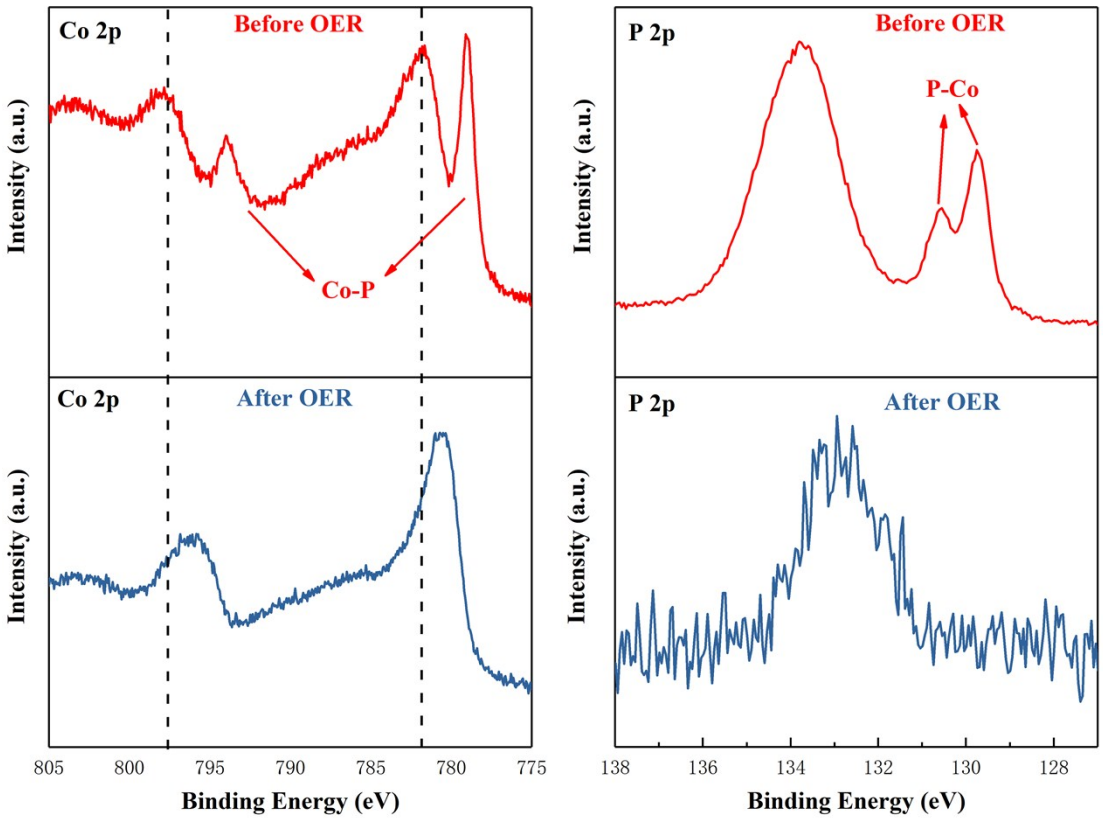

Figure S22. High-resolution Co 2p and P 2p XPS spectra of the CoP-NPC before and after the OER stability test.

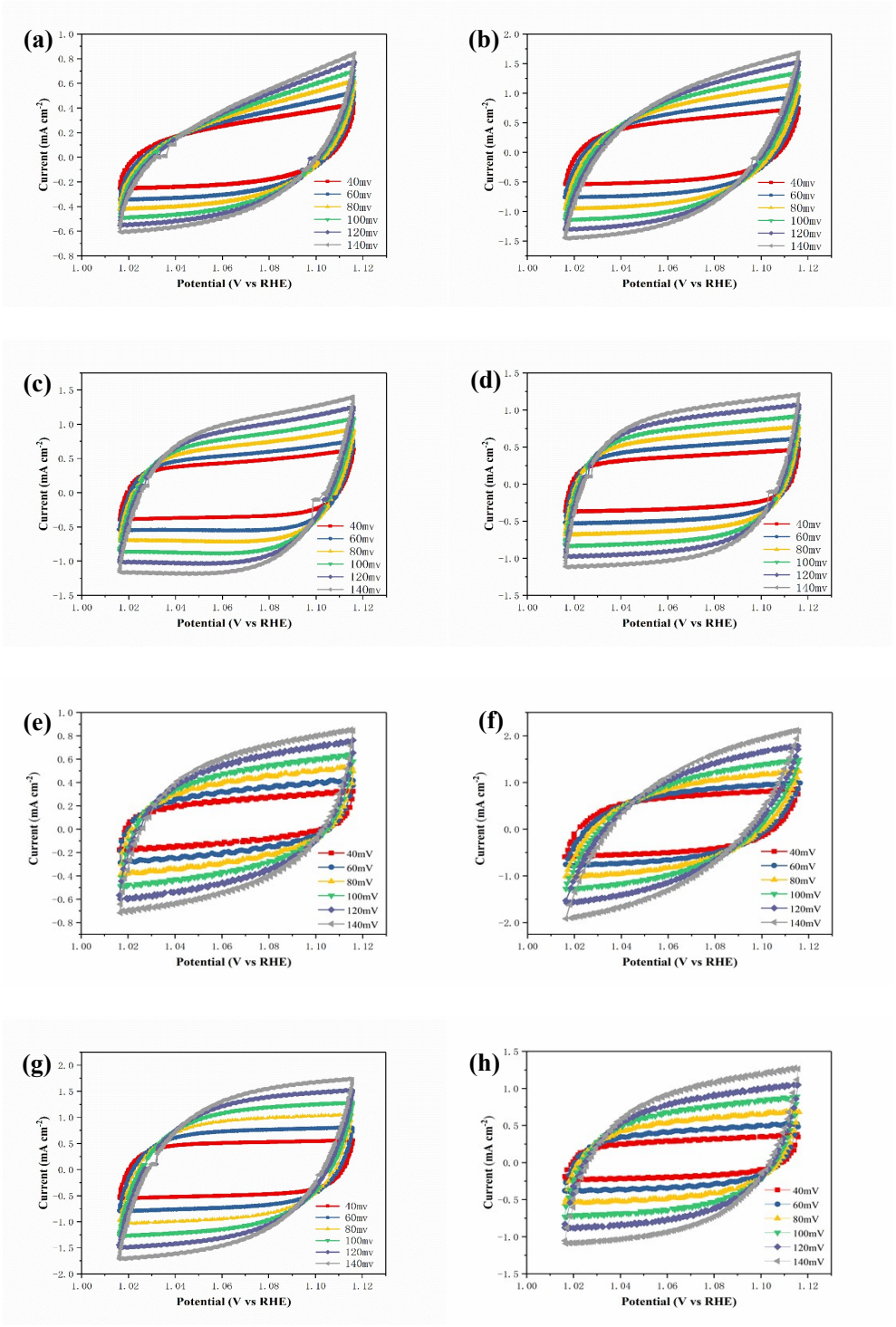

Figure S23. Cyclic voltammograms recorded at various scan rates for (a) Co-NC-600, (b) Co-NC-700, (c) Co-NC-800, (d) Co-NC-900, (e) CoP-NPC-600, (f) CoP-NPC-700, (g) CoP-NPC (CoP-NPC-800) and (h) CoP-NPC-900.

Table S1 The elemental analysis results of the catalysts by XPS

Samples	C (at%)	N (at%)						O (at%)	Co (at%)	P (at%)
		N-1	N-2	N-3	N-4	N-5	SUM			
Co-NC-600	72.2	10.6	6.1	1.8	1.4	0.0	19.9	6.6	1.3	0.0
Co-NC-700	77.6	3.6	4.4	0.3	1.2	0.0	9.5	11.7	1.2	0.0
Co-NC-800	82.4	3.0	2.0	0.6	0.5	0.6	6.7	9.8	1.1	0.0
Co-NC-900	90.8	1.2	1.9	0.5	0.3	0.1	4.0	4.3	0.9	0..0
CoP-NPC	75.4	3.0	2.9	0.6	0.8	1.4	8.7	10.7	1.9	3.3

N-1: pyridinic N ; N-2: pyrrolic N ; N-3: graphitic N ; N-4: oxidized N ; N-5: Co-N_x

Table S2 Elemental compositions of CoP-NPC determined by ICP-OES

Sample	Co (wt%)	P (wt%)
CoP-NPC	19.1	17.5

Table S3 Comparison of the bifunctional OER and ORR activity of CoP-NPC with other electrocatalysts previously reported

Sample	ORR(V): $E_{half\text{-}wave}$	Tafel slope (mV/dec)	OER(V): $E_{j=10}$	Tafel slope (mV/dec)	$\Delta E(V) = E_{j=10} - E_{half\text{-}wave}$	Reference
CoP-NPC	0.82	85	1.54*	58	0.72	This work
Co-NC@CoP-NC	0.78	-	1.56	79	0.78	[1]
CoP-DC	0.81	-	1.55	52	0.74	[2]
Co_2P@CoNPG-900	0.81	69	1.73	93	0.92	[3]
Co-N,B-CSs	0.83	64	1.66	-	0.83	[4]
Co/Co-N-C	0.78	72	1.54*	-	0.76	[5]
Co_3O_4@C-MWCNT	0.81	-	1.55*	62	0.74	[6]
NC@Co-NGC	0.82	51	1.64	91	0.82	[7]
DSNCs CoO/N-graphene	0.81	48	1.57	71	0.76	[8]
NC-Co_3O_4/CC	0.86*	-	1.58*	-	0.72	[9]
Co_4N/CNW/CC	0.80*	-	1.54*	81	0.74	[10]

*means the electrolyte is 1M KOH.

References

[1]Li. X, Jiang. Q, Dou. S, Deng. L, Huo. J, Wang. S, *Journal of Materials Chemistry A,* 2016, **41**, 15836-15840.

[2]Lin. Y, Yang. L, Zhang. Y, Jiang. H, Xiao. Z, Wu. C, Zhang. G, Jiang. J, Song. L, *Advanced Energy Materials*, 2018, **18**, 1703623.

[3]Hao. J, Chang. L, Shen. H, Liu. Y, Li. W, Jie. L, *Electrochimica Acta*, 2017, **231**, 344-353.

[4]Guo. Y, Yuan. P, Zhang. J, Hu. Y, Amiinu. I. S, Wang. X, Zhou. J, Xia. H, Song. Z, Xu. Q, Mu. S, *ACS Nano*, 2018, **2**, 1894-1901.

[5]Yu. P, Wang. L, Sun. F, Xie. Y, Liu. X, Ma. J, Wang. X, Tian. C, Li. J, Fu. H, *Advanced Materials*, 2019, **30**, 1901666.

[6]Li. X, Fang. Y, Lin. X, Min. T, An. X, Yan. F, Rong. L, Jin. J, Ma. J, *Journal of Materials Chemistry A*, 2015, **33**, 17392-17402.

[7]Liu. S, Wang. Z, Zhou. S, Yu. F, Yu. M, Chiang. C. Y, Zhou. W, Zhao. J, Qiu. J, *Advanced Materials*, 2017, **31**, 1700874.

[8]Mao. S, Wen. Z, Huang. T, Hou. Y, Chen. J, *Energ Environ Sci*, 2014, **2**, 609-616.

[9]Guan. C, Sumboja. A, Wu. H, Ren. W, Liu. X, Zhang. H, Liu. Z, Cheng. C, Pennycook. S. J, Wang. J, *Advanced Materials*, 2017, **44**, 1701863.

[10]Meng. F, Zhong. H, Bao. D, Yan. J, Zhang. X, *Journal of the American Chemical Society*, 2016, **32**, 10226-10231.